Review Article

Dyari Mustafa Mamand, Nazk Mohammed Aziz and Rebaz Anwar Omer*

Effect of doping of metal salts on polymers and their applications in various fields

https://doi.org/10.1515/revic-2024-0034
Received May 22, 2024; accepted August 1, 2024;
published online August 29, 2024

Abstract: Transition metal compounds (TMCs) provide the benefits of vast reserves, affordability, non-toxicity, and environmental friendliness, making them highly sought-after in recent times. Integrating transition metal salts into polymers may result in substantial enhancements in optical and electrical characteristics, making them appealing for many applications. Transition metal ions may display a range of electronic transitions, which enables the adjustment of absorption and emission spectra. This characteristic has significant value in applications such as light-emitting devices (LEDs) and sensors. The photoluminescence of polymers may be improved by the addition of transition metal salts, which results in light emission that is both more brilliant and more efficient. On the other hand, this is advantageous for screens and optoelectronic devices. The presence of transition metal salts in polymers may help to improve their optical stability, hence lowering the probability that the polymers will degrade or change color over time. When it comes to the performance of optical devices over the long run, this is quite essential. Elevating the electrical conductivity of polymers is possible via the use of transition metal salts. This is very helpful in the process of developing conductive polymers for use in applications such as electronic fabrics, organic solar cells, and flexible electronic devices. Transition metal salts can affect the electrical band structure of polymers, which enables the band gap of the material to be tuned. This is very necessary in order to maximize the amount of light that is absorbed by photovoltaic devices. Through having all these benefits, we conducted a review to find out the effects on polymeric materials.

Keywords: transition metal; polymer integration; optical and electrical enhancements; photoluminescence; electrical conductivity

***Corresponding author: Rebaz Anwar Omer**, Department of Chemistry, Faculty of Science & Health, Koya University, Koya, KOY45, Kurdistan Region, Iraq; and Department of Pharmacy, College of Pharmacy, Knowledge University, Erbil 44001, Iraq, E-mail: rebaz.anwar@koyauniversity.org. https://orcid.org/0000-0002-3774-6071
Dyari Mustafa Mamand, Department of Physics, College of Science, University of Raparin, Sulaymaniyah, Iraq
Nazk Mohammed Aziz, Department of Chemistry, College of Science, University of Sulaimani, Sulaymaniyah, KRG, Iraq

1 Introduction

Transition metals are classified as elements that occupy the d-block of the periodic table. Transition metals exhibit several oxidation states, enabling them to absorb and catalyze other chemicals.[1] Because of their one-of-a-kind electronic exchange capabilities, transition metal ions or other cations have been used as dopants for the conductive polymer. These dopants have the potential to serve as redox catalysts and corrosion inhibitors in compounds that are composed of polymers. It is usual practice to use transition metals (TM) as dopants due to the fact that they possess a distinctive electronic structure and the capacity to either donate or take electrons.[2] As a result of its ability to change the electrical and structural characteristics of the polymer,[3,4] doping polyaniline (PANI) with transition metals has garnered a significant amount of interest over the last several years. Because it enables novel applications in the fields of energy storage, catalysis, and sensing.[5] The electrical conductivity of PANI may be enhanced by doping it with transition metals, which increases the abundance of free charge carriers. Additionally, Doping may stabilize the structure of the molecules within the polymer, making it more thermally stable.[6] Moreover, the introduction of transition metal ions induces changes in the electronic and structural characteristics of PANI composites, leading to an augmentation in their specific capacitance. This rise is attributed to the creation of a greater number of charge storage sites, ultimately enhancing the electrochemical performance of the composites.[6] In addition, the cycling stability of supercapacitors is enhanced as a result of the presence of transition metal dopants, which stabilize the PANI structure and inhibit undesirable degradation processes over multiple cycles inside the device.[7] The use of

transition metal dopants improves charge transfer kinetics, which in turn allows for quicker charge and discharge rates.[8] Furthermore, PANI composites doped with transition metals have customized features that increase their potential uses in energy storage systems. These qualities may include catalytic or magnetic characteristics brought about by certain transition metals. Transition metals and their compounds have catalytic capabilities that are useful in biomass gasification. Among transition metal catalysts, those derived from nickel (Ni) and iron (Fe) compounds see the greatest use in biomass gasification. There is a mutually beneficial relationship between pyrolysis, oxidation, and Techniques for biodiesel tar reformation cracking tar employing catalysts made of transition metals.[9] In these kinds of reactions, metal catalysts lower the activation energy needed, causing the tar to break more rapidly and thoroughly. When it comes to reducing tar, nickel-based catalysts are head and shoulders above the competition when it comes to converting bio-oil vapors into hydrogen-rich syngas.[10] The use of transition metal catalysts in biomass tar cracking involves a series of processes that work together, including pyrolysis, oxidation, and tar reforming. By lowering the activation energy required for these processes, metal catalysts allow for more rapid and complete tar cracking. When it comes to reducing tar, catalysts based on nickel outperform other options when it comes to transforming bio-oil vapors into hydrogen-rich syngas.[11] These band gap energies were shown to decrease as the NaCl concentration in the PVA matrix increased when salts were applied to polymeric polymers like PVA. Because doping causes the polymer to degrade at a faster rate, we were able to utilize the Urbach index to determine that the samples Urbach energies rose sharply as the NaCl concentration rose. The electrically conductive properties of the PVA/NaCl electrolyte samples were assessed by plotting DC conductivity against the concentration of sodium chloride at room temperature. At a doped concentration of 0.1 g NaCl, the DC conductivity of the produced electrolytes rose to 2.06×10^{-2} S/m. At a doped concentration of 0.5 g NaCl, the DC conductivity climbed to 4.60×10^{-2} S/m. The rise in the number of polarons in the PVA matrix was caused by a higher degree of conjugation of π-orbitals, which led to this increase.[12] The transition metal oxides are a class of semiconductors that have several applications in many different industries, including electronics, catalysis, magnetic storage, and solar energy conversion. Since it is the structural component of several high-temperature superconductors, cupric oxide (CuO) has garnered the greatest attention among these substances.[13] Copper(II) oxide and other P-type semiconductors with band gaps of 1.2–1.9 eV are useful for photothermal and photoconductive applications. Copper oxide, a very efficient catalyst for the oxidation of CO, has found widespread use in indoor air purification systems, fuel cells, and the treatment of vehicle exhaust.[14] Researchers have shown that a copper(II) oxide electrode can insert and extract lithium with great efficiency and good capacity retention, making it ideal for use in rechargeable batteries. This is a fascinating field of research since transition metal sulfides have many interesting optical, catalytic, and electrical properties and applications.[15]

2 Literature review

Salt has been important in many different fields and applications. Because of their different properties, this section lists some important uses of salts. A study conducted to investigate by Ejigu in 2018[16] utilized the catalytic antioxidant properties of several transition metal salts in the electrochemical exfoliation process of graphite. Some transition metals, such as Co^{2+} and Fe^{3+}, have acted as antioxidants to prevent the oxidation of the graphene surface, while others, such as Ru^{3+} and Mn^{2+} possess the ability to decorate using metal oxides. The most notable finding of the result of the investigation, the application of transition metal salts (Co^{2+}, Ru^{3+}, or Ir^{3+}) with metal oxides as effective auto catalysts for oxidative evolution events, led to the production of superior non-oxidized graphene. Cobalt is unique in that it does not modify the performance of graphene. It only functions as a very efficient shield against the surface oxidation of graphite caused by the hydroxyl radical. This results in the production of top-notch non-oxidized graphene with an unusually high carbon-to-oxygen ratio. Calcium chloride and related hydrates are appealing substances for a range of thermal processes due to their hygroscopic nature, cost-effectiveness, relatively low to medium melting points, and heat of hydration. The ammonia sorption is very significant for refrigeration purposes, as proposed by N'Tsoukpoe et al. in 2015.[17] Calcium chloride is a widely used chemical in thermal engineering processes for improving energy efficiency. This material has been utilized in a range of uses, including drying,[18] retrieval of water or its removal through air,[19] applications using phase change materials,[20] closed sorption processes,[21] desiccant refrigeration or dehumidification.[22] The use of a significant amount of electron mediators is necessary for photoelectrochemical cells due to the relatively high concentration of electrolyte, Bignozzi et al. in 2013.[23] Therefore, when selecting and designing the redox couple, it is important to consider cost-effective and readily available metals from the first transition row, as well as easily synthesizable ligands. Currently, octahedral

Co(II)/(III) polypyridine complexes are considered the most effective instances of electron transfer mediators derived from coordination compounds. The Co(II)/(III) pair is often distinguished by a significant inner sphere reorganization energy linked to the electron transfer. This is primarily caused by the participation of a metal-centered e.g., redox orbital with antibonding properties. The transition from high spin Co(II) $t_{2g}^5 e_g^2$ (T_{1g}^4) to low spin Co(III) t_{2g}^6 (A_{1g}^1) may also help to explain the generally low self-exchange rate constants (i.e., 4×10^{-2} $M^{-1}s^{-1}$ for $[Co(phen)_3]^{3+/2+}$) found in many cobalt complexes.[24] Ruthenium complex $[Ru(4,7\text{-}Ph_2\text{-}phen)_3]^{2+}$, often used in the production of an electrochemical cell using an electrochemical redox process, may be utilized as a dopant in a semiconductor polymer layer to create carrier-injection-type light-emitting diodes (LEDs). The Ru complexes possess steady redox characteristics, which provide them an edge over other commonly used metal complexes, Xia et al. in 2004.[25] An electron-to-photon conversion efficiency of 5.5 % was achieved by the use of ruthenium complex in a light-emitting device using this method, by Rudmann et al. in 2003.[26] The maximum phosphorescence quantum yield that has been recorded for ruthenium complexes that comprise replacement 2,2-bipyridine and 1,10-phenanthroline ligands is about 40 percent, Kapturkiewicz in 1995.[27] When compared to traditional electronic devices, organic light-emitting diodes (OLEDs), the compensations of such organizations include their more brightness and efficiency at low operating voltage, as well as the fact that they do not need cathodes with low work function that are low in power (Figure 1).

3 Metal complex structure and formation

3.1 Metal complex formation

Coordination compounds are molecular structures that include one or more metal centers and are attached to ligands, which are atoms, ions, or molecules that transfer electrons to the metal. These structures are referred to as coordination compounds. These compounds have the potential to either be neutral or charged and vice versa.

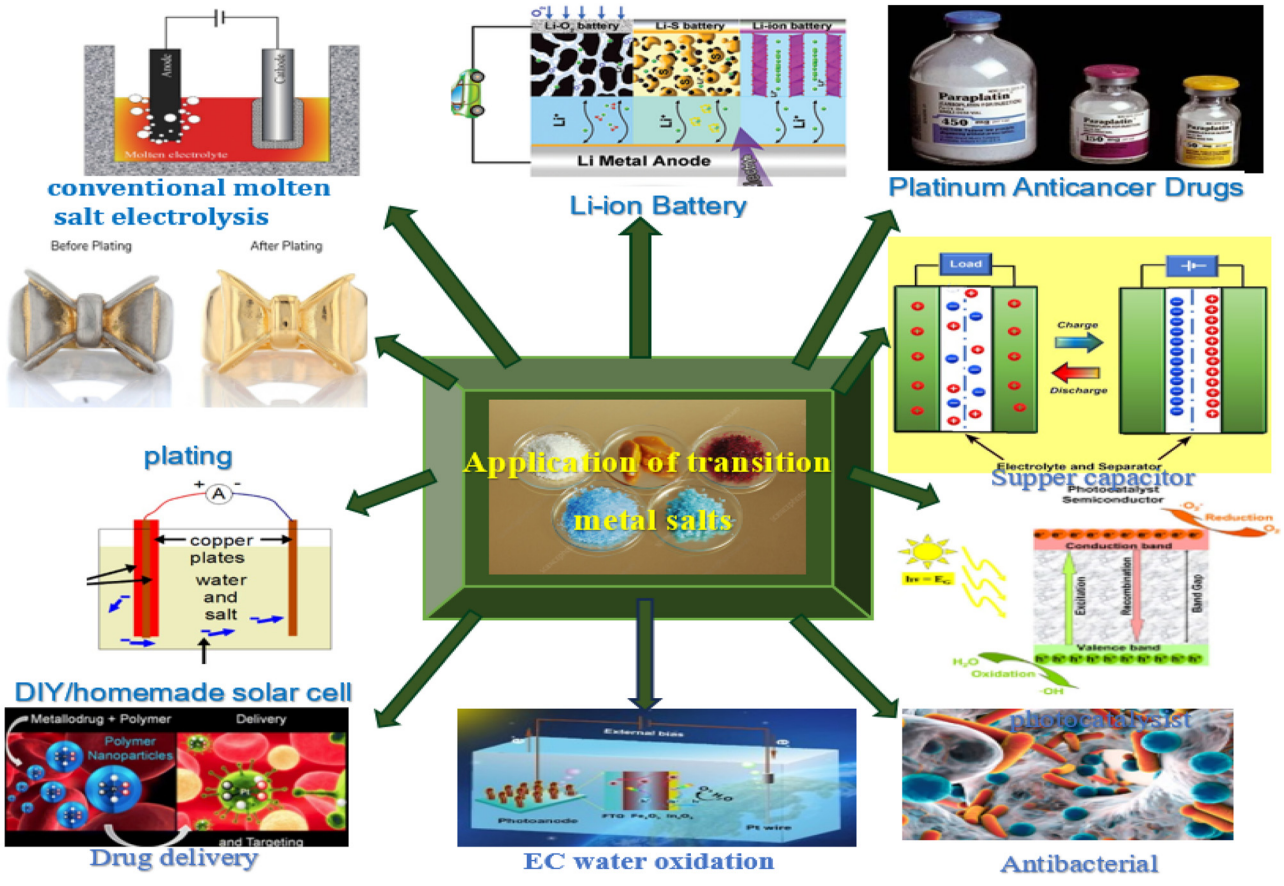

Figure 1: Applications of transition metal salts in various fields.

When the complex is charged, the counter-ions that are situated in close proximity to it serve to stabilize the complex.[28] Complex ions are characterized by the presence of a metal ion at its core, which is encircled by additional ions or molecules. It is possible to think of them being intimately related to one another and the core ion via the connection of coordinate bonds, also known as dative covalent bonds, but, in some instances, the bonding situation is much supplementary complicated than that. "Ligands" in the surrounding of metal ions that could be ions or molecules that are at the center of the molecule. The study of the compounds that appear as a result of the interaction between metals and ligands is known as coordination chemistry. A ligand may be any molecule or ion that forms a bond with the metal.[28] The structure that contains the metal bonded to its ligands is referred to as a metal complex. As an example, the neutral metal complex $[PtCl_2(NH_3)_2]$ is the one in which the Pt^{2+} metal is bonded to two Cl^- ligands and two NH_3 ligands. It is referred to as a complex ion when a complex is charged (complex cation such as $[Pt(NH_3)_4{}^{2+}$). The creation of a molecular structure containing ions containing opposing electric charges allows for the stabilization of complicated ions.

The way chemicals work in coordination makes this possible (ex. $[Pt(NH_3)_4]Cl_2$).[29] Square brackets constitute a common way to describe the procedure for interacting with complicated ions. On the other hand, counterions are written outside of the brackets. By this approach, it is usually acknowledged that ligands that are inserted inside the brackets are immediately linked to the metal ion, and this is situated in the initially formed coordination sphere of the metal and is additionally referred to by the term inner coordination spheres. Aside from their direct bond to the metal, ions stated outside the brackets are presumed to be in the subsequent coordination sphere. Complex Anion: $[CoCl_4(NH_3)_2]^-$, Neutral Complex: $[CoCl_3(NH_3)_3]$, Coordination Compound: $K_4[Fe\ (CN)_6]$, Complex Cation: $[CO(NH_3)_6]^{3+}$. When silver ions combine with neutral ammonia molecules, a common metal complex is formed: $Ag\ (NH_3)^{2+}$.[30]

$$Ag^+ + 2NH_3 \rightarrow Ag\,(NH_3)^{2+}$$

A complex $Ag\,(S_2O_3)_2^{3-}$ this happens when silver ions and thiosulfate ions with a negative charge combine:

$$Ag^+ + 2S_2O_3^{2-} \rightarrow Ag\,(S_2O_3)_2^{3-}$$

How ligands are arranged, and the shape of the metal center determine the characteristics of coordination compounds (Figure 2). Isomers may have vastly varied characteristics while sharing the same chemical formula. There exist molecules known as isomers that have chemical formulas that are identical to one another, yet their atoms are

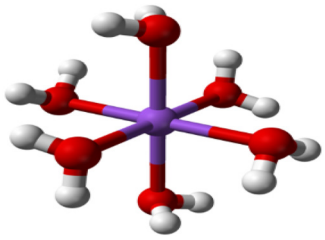

Figure 2: There are six monodentate ligands linked to the central atom (C).

arranged in space differently. The term "geometric isomers" refers to isomers that have their ligands arranged in slightly varied geometric patterns. The term "optical isomers" refers to isomers that have structures that are identical to those of identical isomers.

Complex ions or coordination compounds are formed when metal ions in solution combine with ligands, which might be solvent molecules, other simple ions, or chelating groups. These complexes are distinguished by the existence of a central atom or ion, often a transition metal, and a group of ions or neutral molecules around it. Ligands are molecular ions or neutral molecules that establish a connection with a central metal atom or ion. At the same time as the central atom performs the role of a Lewis acid (an electron pair acceptor), ligands perform the function of Lewis bases (electron pair donors). At a minimum, ligands consist of a donor atom that has an electron pair that is used for the formation of covalent connections with the center atom. It is possible to interpret the word "monodentate" as "one tooth", which refers to the fact that the ligand binds to the center of the tooth via just one atom. A monodentate ligand is characterized by the presence of a single donor atom that is associated with the central metal atom or ion. The following are some examples of monodentate ligands: chloride ions (which are referred to as chloro when they are a ligand), water (which is referred to as aqua when it is a ligand), hydroxide ions (which are referred to as hydroxo when they are a ligand), and ammonia (which is referred to as ammine when it is a ligand).[31]

Bidentate ligands are able to attach to a central metal atom or ion at two different places within the molecule because they include two donor atoms. A few of the instances of bidentate ligands frequently appear such as ethylenediamine (en) and the oxalate ion (ox).[32] A schematic of ethylenediamine can be seen in the following: For each of the nitrogen (blue) atoms on the borders. Additionally, two electrons are free with the purpose of establishing a link with a metal atom or ion in the center of the molecule.

The total amount of atoms that are employed trendy the construction of a bond to a central metal atom or ion varies

among polydentate ligands. One instance of a polydentate ligand is EDTA, which is a hexadentate ligand. This ligand has six donor atoms that are equipped with electron pairs that may remain utilized to establish a connection between a central metal atom or ion.

The ambidentate ligands, in contrast to the polydentate ligands, are able to connect to the central atom in two different locations. An excellent illustration of this is thiocyanate, often known as SCN^-, which may connect to either the nitrogen atom or the sulfur atom with equal ease.

A ring is constructed by the process of chelation, which also entails the attachment of a polydentate ligand to a metal ion. Chelation is a relatively new technique. Following this technique, a complex, which is commonly referred to be a chelate, is formed, while the polydentate ligand is considered to function as a type of chelating agent. The chelate is formed primarily as a consequence of the technique mentioned above. In 1920, Sir Gilbert T. Morgan and H.D.K. Drew were the first people to use the word "chelate". They asserted that the phrase was first used.[33] It is recommended that the chelate characterized be employed to describe the caliper-like groupings that function as chemical two-attachment constituents and connect to the central atom to build heterocyclic rings. This term originated from the huge claw, also known for its shape chela (chely in Greek), that is seen on lobsters along with other crustaceans.

In comparison to ligands that only contain a single binding group, which are referred to as monodentate ligands (which means "single tooth"), chelating ligands possess a far higher affinity for metal ions: this is what the term suggests. A few examples of chelating compounds are ethylenediamine (shown in Figure 3) and ethylenediaminetetraacetic acid (shown in Figure 4). The macrocyclic impact makes use of the same fundamental concept as the chelate impact; however, the cyclic structure of the ligand contributes to an even greater enhancement of the impact. Not only are macrocyclic ligands multi-dentate, but they also allow for less flexibility in conformation they are covalently confined to their cyclic shape. There is little entropy cost when the ligand encircles the metal ion since it is "pre-organized" for binding. Hemoglobin contains the transition metal ion Fe^{2+} and is bound to four different locations on its cyclic ligand, heme b (Figure 5).[34]

- When metal ions are coordinated via two oxygen atoms, the resulting ligand is acetylacetonate, also known as $acac^-$, on top. Since it is a hard base, $acac^-$ likes cations that are also hard acids. $Acac^-$ produces neutral, volatile compounds with divalent metal ions, such as $Cu(acac)^2$ and $Mo(acac)^2$, which are used in the process of chemical vapor deposition (CVD) for the production of metal thin films.-

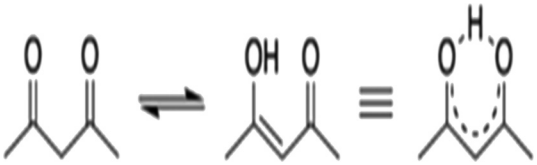

- 2,2′-Bipyridine (Bipyridine) The compound known as 2,2′-Bipyridine, which is shown on the left side of Figure 5, along with similar bidentate ligands like 1,10-phenanthroline, may form propeller-shaped complexes with metals like Ru^{2+}. Both photocatalysis and synthetic photosynthesis might benefit from the $[Ru(bpy)^3]^{2+}$ complex since it is photoluminescent and can also conduct photo-redox reactions. This makes it an intriguing chemical for both of these applications.[35]
- Crown ethers, which include 18-crown-6 2,2′-Bipyridine (shown in the middle of Figure 5), are cyclic hard bases that can complex alkali metal cations. The quantity of ethylene oxide units present in the ring determines whether or not crowns have the ability to bind Li^+, Na^+, or K^+ preferentially.
- The chelating capabilities of crown ethers are similar to those of the natural antibiotic valinomycin, which is 2,2′-Bipyridine (Figure 5: right). Valinomycin preferentially ferries K^+ ions through the cell membranes of bacteria and ultimately results in the death of the bacterium by squandering its exterior membrane potential. A cyclic hard base, valinomycin, is similar to crown ethers in their structure.

3.2 Anionic complexes of metals

Anionic compounds of metallic substances in widespread oxidation states. Among the alkynyl complexes that have been identified at this point, the anionic acetylides of

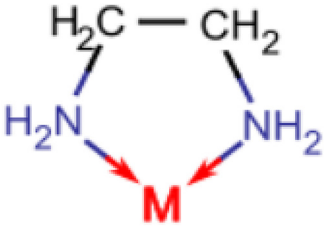

Figure 3: An example of a bidentate ligand is the compound known as ethylenediamine (en). Ethylenediamine, often known as en, is a bidentate ligand that, when coordinated to a metal ion M, forms a ring with five members.

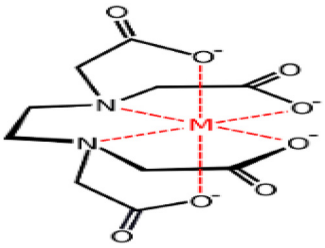

Figure 4: On the left is an unbound EDTA ion, while on the right is EDTA that has been attached to a typical transition metal. Ethylenediaminetetraacetic acid, often known as EDTA, is a hexadentate ligand that can bind a metal via many "teeth".

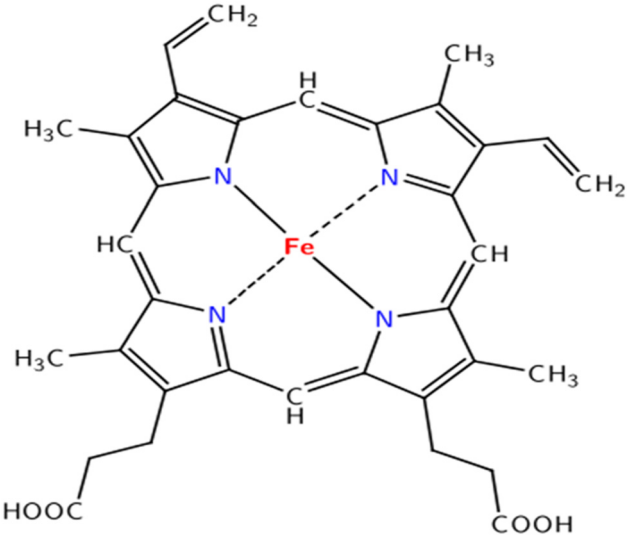

Figure 5: A macrocyclic ligand known as heme b may bind iron to hemoglobin.

d-metals and group IB and IIB metals (Table 1) exhibit the highest level of reactivity. These compounds show a high degree of protolysis. This is as a result of the high basic nature of the alkynyl ions as well as the anionic structure of the complex ions. A significant number of the solid compounds, which are mainly unable to dissolve in the typical organic solvents, detonate upon collision provided their center atoms contain d-orbitals that are either full or 50 percent occupied. As a result of all of these characteristics, the arrangements that have been suggested for the complex anions are fully dependent on the magnetic and infrared measurements of the constituent solids.[36]

With the possible exception of the high-spin complex acetylides of manganese(II) and the low-spin complexes of the same kind $[Co(C_2R)_6]^{4-}$, These compounds are distinct when compared to low-spin cyano complexes $[Mn(CN)_6]^{4-}$, $[Co(CN)_5]^{3-}$ and $[Co_2(CN)_{10}]^{6-}$ correspondingly,[50] In every respect, the complex cyanides and the anionic alkynyl complexes are identical in terms of their stoichiometry,

Table 1: Electron configurations d^n and magnetic moments μ_{eff}(B.M) of "common-valent" metals in anionic complex acetylides.

Complex	d^n	μ_{eff}(B.M)
$K_3[Cr(C_2H)_6]$[37]	3	5.9
$K_3[Mn(C_2H)_6]$[38]	4	
$M_2[Mn(C_2R)_4]$ (M = K, R = H)[39]	5	5.9
$K_3[Fe(C_2H)_6]$[40]	5	
$K_4[Fe(C_2H)_6]$[41]	6	0
$Na_3[Co(C_2H)_6]$[42]		
$[Pph_4]_3Na[Co(C_2H)_6]$[43]		
$K_2[Ni(C_2H)_4]$[44]		1.8
$Li_2[Ni(C_2\ pH)_4]$[45]	8	0
$K_2[Pd(C_2H)_4]$[44]		
$K_2[Pt(C_2H)_4]$[44]		
$K_2[Cu(C_2H)_3]$, $K[Cu(C_2H)_2]$[46]		
$K_2[Zn(C_2H)_4]$[47]		
$K[Ag(C_2H)_2]$[48]	10	0
$[Cu(H_2O)_2(nmen)_2](tdc)$[49]	–	1.61
$[Cu(tdc)(nmpen)_2]$[49]	–	1.52

color, and magnetic properties. There is a possibility that the dinuclear gold(I) complexes share comparable characteristics $[Pph_4]_2[RC_2Au–C\equiv C–AuC_2R]$ and $[Pph_4]_2[NCAu–C\equiv C–AuCN]$.[51] The idea that these compounds' anions are linear and include end-on bridging C≡C groups is supported by the spectrum of vibrations of these compounds. Presumably, there are bridges of similar type inside the endless chains –Ag–C≡C–Ag–C≡C– of the polymeric $[KC\equiv CAg]_n$,[48] comparing favorably to chains that are linear Ag–C≡N–Ag–C≡N– of the polymeric $[AgCN]_n$.[52] As a result of a redox reaction, the preparation of anionic acetylides of the d^9-metal copper(II) was unsuccessful (1).[46]

$$2[RC\equiv C]^- + 2Cu^{2+} \rightarrow 2Cu^+ + RC\equiv C - C\equiv CR$$

Similar to the previous example, the redox reaction (2) presents a challenge when it comes to the synthesis of alkynylpentacyanoferrates (III).[53]

$$2[RC\equiv C]^- + [Fe(CN)_5NO_2]^{3-} \rightarrow [Fe(CN)_5NO_2]^{2-} + RC\equiv C - C\equiv CR$$

An assortment of combined anionic complex acetylides, among which are the low-spin compounds, were, despite this, capable of being isolated cis-$Na_2[Co(C2H_4)(Pet_3)_2]$, trans-$Na_2[Co(C_2H)_4(Pph_3)_2]$, trans-$Na_2[Co(C_2Ph)_4(Pet_3)_2]$, trans-$[Pph_4]Na[Co(C_2ph)_4(Pph_3)_2]$,[54] $K_2[CoC_2cy)_4(NH_3)_2$, the diamagnetic complexes trans-$Ba[Pd(C_2R)_2(CN)_2]$ (R = H, ph)[55] and trans-$K_{2n}[Pt(C_2R)_4(dpe)]_n$. (R = H, me, ph).[56] The geographical demands of R and R′ are responsible for determining the configuration of the anions $[Co(C_2R)_4(PR)_2]^{2-}$ Furthermore, the polymeric character of $[Pt(C_2R)_4(dpe)]_n^{2n}$ seems to be produced by dpe bridges. The infrared spectrum

of the likely planar anions $[Pd(C_2R)_2(CN)_2]^{2-}$ are more consistent with a trans-structure than they are with a cis arrangement of the ligands, which was the hypothesis that was previously put up. It is also possible for phenyl acetylide ligands to partly substitute for the cyano ligands that are associated with the "nitroprusside" ion. Nevertheless, the products of the reaction $[Pph_4]_2[FeC_2ph)(CN)_4NO]$ and $[Pph_4]_2[FeC_2ph)(CN)_2NO]$ Thermally, they are not stable enough for structural characterization, and they are considerably less stable compared to the diamagnetic component trans-$K_4[Fe(C_2cy)_2(CN)_4]$.[57] The latest study has demonstrated the fact that the phthalocyanines of certain d-metals, when combined with one or two phenyl acetylide ligands, may result in the formation of anionic complexes that are characterized by their vivid colors $Li[M(C_2ph)(pc)]$. *n* THF (M^{III} = Cr, Co; *n* = 5,4), $Li[Mn(C_2ph)(pc)]$. 4.5 THF, $Li_2[Fe(C_2ph)_2(pc)]$. 7 THF, $Li_2[Co(C_2ph)(pc)]_2$. 8 THF and Na $[Zn(C_2ph)(pc)]$ – 5 THF. The magnetic properties of the complexes that include all of the additional metals, except the cobalt(II) combination, are remarkably comparable to those of the equivalent complexes listed in Table 1. On the other hand, the cobalt(II) complex is diamagnetic, and as a result, it is thought to be dimeric due to the interaction between cobalt and cobalt. In recent years, it has been reported that the initial complex acetylides of tervalent f-metals are complexes of the kind that are dependent on temperature and humidity $LiM(C_2R)_4(THF)_x$ (M = Eu, Er, Yb, Lu; R = bu, t-bu; *x* = 0–1).[58] Particularly about alkynyl complexes of primary group metals, there are just a few thallium(III) complexes of the sort that are of importance $[Pph_4][Tl(C_2R)_4]$ (R = me, ph) remain recognized at current.[59] These electrolytes with low ionization strength undergo protolysis readily and do not exhibit explosive properties.

3.3 Anionic complexes of metals in low oxidation states

Alkynyl anions are equally as effective as the cyanide ion when it comes to becoming ligands to stabilize low oxidation states of the core d-metal atoms. In the process of creating alkynyl and cyano complexes, accordingly, which include technically zerovalent nickel, palladium, and platinum, this is demonstrated. Obtaining both of these diamagnetic combinations is accomplished by the reduction of the metalates involved (II) $[M(C_2R)_4]^{2-}$ and $[M(CN)_4]^{2-}$ correspondingly (M = Ni, Pd, Pt) using liquid ammonia and alkali metals. The identical procedure produced the tris(phenylethynyl)cuprate(0) $Ba_3[Cu(C_2ph)_3]_2$ dimerization of the anions via Cu–Cu bonds is used to explain their diamagnetism. These compounds all happen to be somewhat pyrophoric and exceptionally reactive to oxygen and water. Therefore, the infrared measurements of the solids provide the only basis for the anion geometries that have been presented. The diamagnetic complexes $K_3[M(CO)_3(C_2R)_3]$ (R = H, me, ph; M = Cr, MO, W) are quickly proteolyzed and have a pyrophoric component to some extent.[60] There continues to be a lack of clarity on the coordination geometry of their anions. Upon doing a thorough examination of the characteristics of the anionic complex acetylides, it is discovered that the progression through which they undergo protolysis indicates to be contingent upon the electron configuration of the central metal atom. Acids release the alkynes RC≡CH from complexes with the high-spin d^5-metal manganese (II) and d^{10}-metals of groups IB and IIB, while protolysis of any additional complexes also generates unknown organic compounds via side reactions. Combinations of the appropriate alkynes and related hydrogenated derivatives are produced by the protolytic breakdown of the "zerovalent" d^{10}-metal compounds $RCH{=}CH_2$, RC_2H_5 beyond chemicals that resemble tar. Because complex cyanides and acetylides do not adhere rigidly to the l8 electron rule, it is clear that these two classes share many coordinative properties.

4 Applications of metal salt doping in various fields

4.1 Polymer with salt complexes for batteries

One viable option for the safe and stable storage of high-energy electrochemical energy is solid-state lithium metal batteries based on polymer electrolytes. In addition, the overall performances of solid-state lithium metal batteries have been heavily influenced by the interface contact between the electrolyte and electrodes, as well as the inherent features of polymer electrolytes.[61] Enhanced compatibility and assembly of batteries are achieved by the use of the *in-situ* polymerization technique, which ultimately leads to enhanced performance. With the help of this method, it is also feasible to resolve the problems with interfaces that are present among the polymer electrolyte the cathode, and the anode. Some of the techniques that are included include those that stabilize the interface contact and lower resistances. An electrolyte that is often referred to as a "salt-in-polymer" is a polymer that includes salt complexes. This term is commonly used in the context of batteries. As seen in Figure 6a, Armand[62] were the ones who first introduced this idea. There is a connection between the segmental motions of polymer chains and the ion transport mechanism that is present in this specific kind of polymer

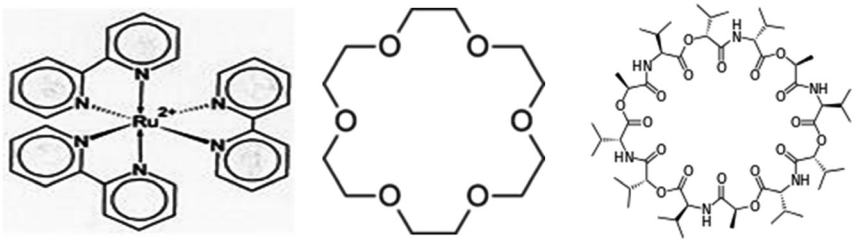

Figure 6: (Left) 2,2′-Bipyridine, (center) 18-crown-6 2,2′-Bipyridine (right) valinomycin.

electrolyte. Free volumes are created as a result of these movements, which make it possible for ions to move about in a way that is coordinated with polar groups.[63,64] In the context of this discussion, the polar groups are known as functional groups. These groups are composed of carbon monoxide, carbon dioxide, carbon monoxide, and other comparable components. The chemical properties of organic molecules are determined by these atoms or groups of atoms, which are responsible for providing the information. On the other hand, functional units are not the same thing as functional groups; rather, they are the intermediary structural units that provide particular functions between the atomic/molecular size and the macroscopic scale. Additionally, the "salt-in polymer" electrolyte must have a low glass transition temperature (T_g) in order to function properly.

Similarly, as seen in Figure 7b, the "polymer-in-salt" electrolyte has been suggested as a means of enhancing ionic conductivity. This is accomplished by incorporating a high concentration of lithium salt (more than 50 percent weight) into the polymer matrix, which allows for a reduction in the T_g.[65,66] The micro-Brownian motion of segments in polymer chains is connected to the ion transport in an electrolyte that is referred to as "polymer-in-salt".[67] This motion occurs above the crystallization or melting transition temperature. Furthermore, the evaluation of the polymer electrolyte necessitates the consideration of the lithium-ion transference number, also referred to as tLi^+. The presence of a large number of negatively charged ions in the electrolyte has been shown to be linked to a small number of lithium ions, as evidenced by previous research.[68] The tLi^+ value for the "salt-in-polymer" electrolyte is below 0.5,[69] making it easy to create a concentration gradient near the electrode. This may lead to the occurrence of high-concentration polarization in polymer electrolytes, potential polarization in the battery, and unavoidable side reactions between the electrolyte and the electrode. Enhanced performance of the battery, reduced concentration polarization of electrolytes, and controlled anion circulation within the polymer matrix are all possible outcomes of using the "single-ion-conducting" polymer electrolyte. This is achieved by the presence of tLi^+ up to be1[61] (Figure 7c). In addition, ion transport in the polymer electrolyte occurs via a hopping process between anionic sites that are attached to the polymer chains. This results in a significant reduction in the mobility of the anions.

4.2 The role of Pt in anticancer

The H spin-echo NMR method was utilized to investigate the relationship between cis- and trans-$[PtCl_2(NH_3)_2]$ and glutathione throughout red blood cells that were not damaged. When trans-$[PtCl_2(NH3)_2]$ was added to a suspension of red cells, there was a steady drop in the strength of the resonances for free GSH. Additionally, additional peaks were identified, which may be attributed to the coordination of GSH protons in trans-$[Pt(SG)Cl(NH_3)_2]$, trans-$[Pt(SG)_3(NH_3)_2]$, and possibly the S-bridged complex trans-$[\{(NH_3)_2PtCl\}_3SG]^+$. Noticed as the intensity of the

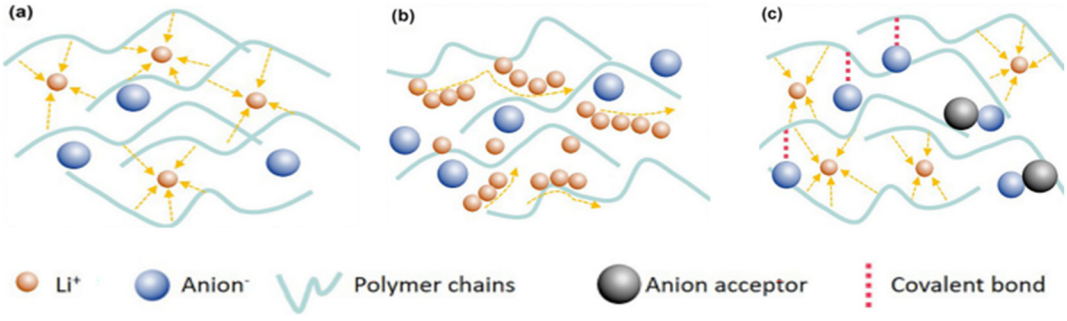

Figure 7: Various polymer electrolytes' ion migration methods shown in schematic diagrams: (a) "salt-in-polymer", (b) "polymer-in-salt" and (c) "single-ion conducting.

resonances for free GSH decreased. The confirmation of the development of trans-[$(Pt(SG)_2(NH_3)_2$] inside the cell was obtained from the ^{1}H NMR spectrum of hemolyzed cells. These cells were ultrafiltered to exclude big molecules of protein. The use of selective-decoupling studies determined the ABM multiplicity of the concerted GSH cys-βcH_2 protons. There is evidence that the mixture complex trans-[Pt(SG)(S-hemoglobin)$(NH_3)_3$] is correspondingly a key metabolite of trans-[$PtCl_2(NH_3)_3$] throughout red cells. The ultrafiltration membrane was able to hold onto 70 % of the entire intracellular glutathione. A slower reaction occurred between cis-[$PtCl_2(NH_3)_3$] and intracellular GSH; following a four-hour incubation, only 35 percent of the GSH had been complexed, in contrast to the 70 percent complexation that occurred with the tens isomer.[70] Despite the fact that there is a substantial amount of data to suggest that the anticancer action is the consequence of their binding to DNA and their prevention of replication,[71] There is a lack of knowledge on the composition of the metabolites of cisplatin which are produced in living organisms, as well as the question of whether or not these byproducts are accountable for the nephrotoxic effects of the drug. The huge number of possible ligands that are present in anatomical structures and are capable of undergoing ligand-exchange reactions is a significant challenge when attempting to identify important metabolites with cis-[$PtCl_2(NH_3)_2$]. *In vivo*, characterization of the metabolites of complex metal compounds is difficult to do due to the limited number of approaches that are currently available.[71] High-pressure liquid chromatography (HPLC) is one method that was previously used in the process of separating low-molecular-weight platinum compounds from plasma.[72] However, it would seem that there have been no prior efforts made to investigate the metabolites of cisplatin inside cells that have not been damaged.

4.3 $Mg(NO_3)_2$ doped CS/MC

In previous research, a polymer mixture consisting of chitosan (CS) and methylcellulose (MC) was subjected to varying weight percentages of magnesium nitrate that was added to the mixture. The preparation of the polymer electrolyte films was accomplished through the usage of the solution casting technique. When it comes to the host matrix, the polymer mix is made up of 70 weight percent of CS and 30 weight percent of MC. Through the use of FTIR analysis, the interactions that took place between the mixture and the $Mg(NO_3)_2$ salt were uncovered. As shown in Figure 8, The electrolyte samples were found to be amorphous, as shown by the relaxation of the XRD peaks and the subsequent crystal computation. Rendering to the findings of the valuable technique of electrical impedance spectroscopy, the influence of carrier concentration was responsible for the reduction in collective resistance that occurred as the amount of salt in the sample increased. $Mg(NO_3)_2$ was present in the sample at a weight percentage of 30 percent. Through the use of EIS analysis, it has been ascertained at room temperature that the maximum DC conductivity is 2.12×10^{-5} S/cm^{-1}. The stability of 3.65 V was discovered to be the greatest conducting film capacity that has been discovered. There was evidence that demonstrated that the ion transport number was 0.86. The efficiency of the Mg ion battery remained before being tested afterward, it had been carried out using the polymer electrolyte that showed the best level of performance. Taking this into consideration, his study suggests an electrolyte that is ideal for an electrochemical vibe that is also practical, inexpensive, and favorable to the environment.[73]

4.4 Effect of metal salts on optical properties

Metal salts, when used as doping, can change all the optical properties of polymers. When $CuCl_2$ is doped into cellulose, the properties of the polymer change.[74] It has been determined that the lowered bandgap energy is the most essential characteristic. In order to measure the basic optical characteristics, for instance, the optical energy gap (E_g), and both the optical dielectric constant's real part (ε_r), and imaginary part (ε_i), loss it has been shown that the quantity of $CuCl_2$ contributes significantly to the effectiveness of these parameters. Calculating both the direct and indirect E_g was accomplished by the use of Tauc's relation. The addition of 20 weight percent of $CuCl_2$ salts resulted in a significant decrease in the bandgap energy of uncontaminated Methy cellulose, which went from 6.21 eV to 2.68 eV. As shown in Figure 9, the optical spectrum, which is the most straightforward and straightforward method for investigating the band structure of solid material, was used to determine the influence that the concentration of $CuCl_2$ had on the optical characteristics of MC. The semi-crystalline structure of MC is shown by the presence of a prominent absorption edge at 244 nm, which is a characteristic of the absorption spectra of pure MC film. The strength of the sharp absorption edge grows, and it shifts towards redshift) longer wavelengths as the concentration of $CuCl_2$ in the composite films increases. This happens because the edge shifts toward longer wavelengths. This shift takes place as a consequence of the progress of strain and the production of an imperfection, which ultimately leads to a reduction in the energy gap measurement of the films that have been made.

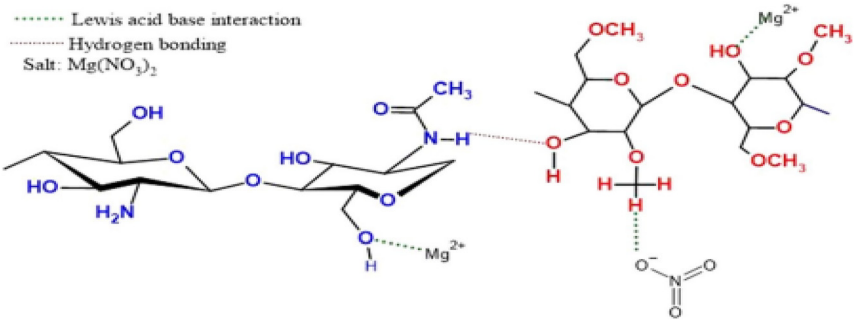

Figure 8: Imaginable chemical interaction arrangement of $Mg(NO_3)_2$ with the poly-blend CS:MC.

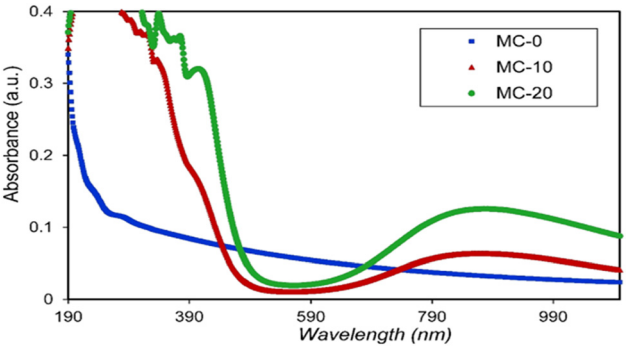

Figure 9: Pure methylcellulose and methylcellulose doped $CuCl_2$ PC films UV–vis spectrum.

Due to the fact that it has a direct connection to the physiochemical and molecular characteristics, another valuable parameter is the refractive index (n) is the most essential optical limitation for optoelectronic applications. There exists a tight connection between the band structure of the material and the dielectric function. The optical spectroscopic approach is an effective tool for determining the band structure of a material because of its aptitude to analyze the substantial. The changes are detailed in the table that follows. When methylcellulose is used as the material for the polymer, metal salts are doped into the polymer in varying amounts. The results of the $CuCl_2$ impact on the samples are consistent with the appearance of additional diffraction peaks, and the strength of these peaks decreases as the concentration of $CuCl_2$ increases. When the amount of $CuCl_2$ in the sample increased, there was a shift in the absorption edge to a side with a lower photon energy. Based on the data shown in Table 2, the rate of the optical E_g for each of the films that were synthesized decreased as the amount of $CuCl_2$ increased. An increase in the Urbach energy (E_o) of PC is produced with the addition of $CuCl_2$, which is associated for a high quantity of tail-to-tail transitions that are conceivable. There was a rise in the refractive index, which went from 1.44 to 2.04.

Table 2: Variation optical properties of methylcellulose after doped $CuCl_2$.

Films	Absorption edge (E_a) (eV)	Refractive index (n)	Direct E_g (eV)	Indirect E_g(eV)	E_g from (ε_i versus hv) (eV)
MC–0	5.58	1.44	6.21	5.7	6
MC-10	2.65	1.66	3.2	2.39	2.69
MC-20	2.5	2.04	2.68	2.3	2.54

4.5 Polyaniline doped with Li salt as an electrode

Due to its rapid charge-discharge kinetics and doping-undoing process, conducting polymer is a very promising material in polymer-based redox supercapacitors. When compared to supercapacitors made of metal oxides, conducting polymers may often be purchased for much less money. Because of its facile processability, controlled electrical conductivity, and environmental durability, polyaniline has garnered a lot of interest among conducting polymers. As an electrode material in a polymer redox supercapacitor, polyaniline powder that had been doped with $LiPF_6$ was employed. After undergoing a chemical preparation process, the polyaniline powder that has been doped with $LiPF_6$ is used as an electrode material in symmetric redox supercapacitors. To be more specific, the electrode sheet is manufactured by depositing the slurry that is made up of polymer, conductor, and binder directly on a charge collector. It was determined that the performance of the polymer electrolyte and the porous polyolefin separator were comparable. Li-doped PANI electrode sheet has an electrical conductivity of 1.7 S/cm, while the ionic conductivity of polymer electrolyte is f 3×10^3 S/cm.

Both of these values are measured in micrometers. Comparative analysis is performed between the performance of a polymer electrolyte and that of a redox supercapacitor that makes use of a polyolefin filter. During

the first discharge, the specific capacitance of a redox supercapacitor that makes use of a porous separator is f 100 F/g, and after 5,000 cycles, it is maintained at 70 F/g. As the number of cycles increases, the discharge capacitance continues to drop in a steady manner. According to the polymer electrolyte, the specific capacitance is f 80 F/g during the first discharge, and it remains at f 60 F/g after 5,000 cycles have been completed. Some individuals have proposed that there is a connection between the electrical conductivity of a salt solution and the mobility of ions that have been dissolved in the solution. The reason for this is that ion movement to opposite electrodes is a fundamental need of voltaic cells and chemical batteries, which produce electricity by decreasing one substance and ionizing another.

In contrast, an electric circuit, like that which lights a bulb, is completed when a voltage is applied to a solution through two electrodes; however, this process does not involve an oxidation-reduction reaction and does not cause the voltage to decrease over time. The only function of the solution is to transfer energy through it. Like metallic electrical connections, the conductivity of frozen salt solutions varies with temperature. On the flip side, liquid salt solutions retained their conductivity and even enhanced it as the temperature rose, making them ideal electrical circuit conductors. A connection occurs between the magnitude, concentration, and charge of the electrolyte cation, all of which affect conductivity.[75]

4.6 Cu(II) complex doped polyaniline (PANI)

Aniline is one of the most important polymers because of its widespread use. Through the doping of metal salts, it has been possible to characterize. $CuSO_4{\cdot}5H_2O$, $[Cu(NH_3)_4]SO_4$, $[Cu(en)_2]SO_4$ and $[Cu(en)_3]SO_4$ has been used as dopants. The UV–vis spectra of the polyaniline doped transition metal has been investigated such as EB-PANI, HCl-PANI and PANI doped through copper Cu^{2+} ion, while the ligands are not the same is presented in Figure 10A and B. Around a wavelength of 634 nm, the benzenoid to quinoid electronic transition from HOMO to LUMO excitation transition, also known as BQET, could be observed between the undoped Polyaniline polymer material. With PANI, which had been doped with HCl, this peak vanished. However, during the process of becoming doped by the Cu^{2+} ion, these peak experiences a blue shift, moving from 634 nm to the region of 533–573 nm. A comparable decrease in wavelength or blue shift was also described by Chen et al.[76] Throughout the process of doping PANI, researchers utilized a variety of transition metal ions, one of which was Cu^{2+}. Higuchi et al.[77] It was determined that the complexation of the Cu^{2+} ion using polyaniline was responsible for this particular blue shift and Chen et al.[76] Moreover, this alteration was linked to the interplay between polyaniline backbones and transition metal ions. The measured blue shift may be ascribed to the connection of the Cu^{2+} ion with the polyaniline, in addition to the observed partial oxidization of the polymer backbone.[78]

Additionally, it was discovered that this displacement was contingent upon the dimensions or voluminosity of the ligands that surround the Cu^{2+} ion. Figure 10B demonstrates that when the size of the ligands increases, the blue shift becomes less. The reduced efficiency of Cu^{2+} ion complexation using polyaniline is attributed to the steric hindrance induced through the presence of bulky ligands around the Cu^{2+} ion. The level of concentration of the doping agent also affects the magnitude of the blue shift. In the case of the identical ligand, it was noticed that the blue shift was bigger when the amount of the doping agent was greater. The fact that the quantity of the dopants had been altered for the identical ligand (as shown in Figure 9B–E) makes this observation very clear. A bigger blue shift appeared when the efficiency of the amount of doping increased with increasing dopant concentration. The π–π* transition in the benzenoid rings is responsible behind the additional absorption peak at 329 nm that was seen in the undoped PANI.[79,80] Upon doping, the π–π* peak causes increases wavelength a red shift, causing it to move to the polaronic area, which spans from 348 to 377 nm. A connection exists between this peak and the production of polaron as well as the level of doping.[81] Because the strength of this peak is at its highest for HCl-PANI, it indicates that there is a significant amount of doping. A reduction in the magnitude of the polaronic peak occurs if there is a rise in the bulkiness of the ligands surrounding the Cu^{2+} ions. It may be seen clearly in Figure 10, namely in plots C, C_1, C_2, and C_3, with $CuSO_4{\cdot}5H_2O$, $[Cu(NH_3)_4]SO_4$, $[Cu(en)_2]SO_4$ and $[Cu(en)_3]SO_4$ as dopants correspondingly. The steric impedance was higher when the ligand size was higher, while the degree of doping was lower when the ligand size was smaller. In addition, Nikolaidis et al. reported a rise in the strength of the polaronic peak after the doping of EB-PANI using CuCl2[82] from EPR studies. It can be seen that the polaronic peak for HCl-PANI is located at 377 nm, but the polaronic peak for compounds C, C_1, C_2, and C_3 is located at 359 nm, 355 nm, 354 nm, and 348 nm, correspondingly. This indicates the shift in the direction of the polaronic region is less pronounced for higher ligand sizes. The fact that the peak in the region of 348–377 nm was connected to the doping amount which provided more evidence was shown in Figure B, C & D where $CuSO_4{\cdot}5H_2O$, $[Cu(en)_2]SO_4$ and $[Cu(en)_3]SO_4$ were used as dopants. When the concentration of the dopant was raised, it was discovered

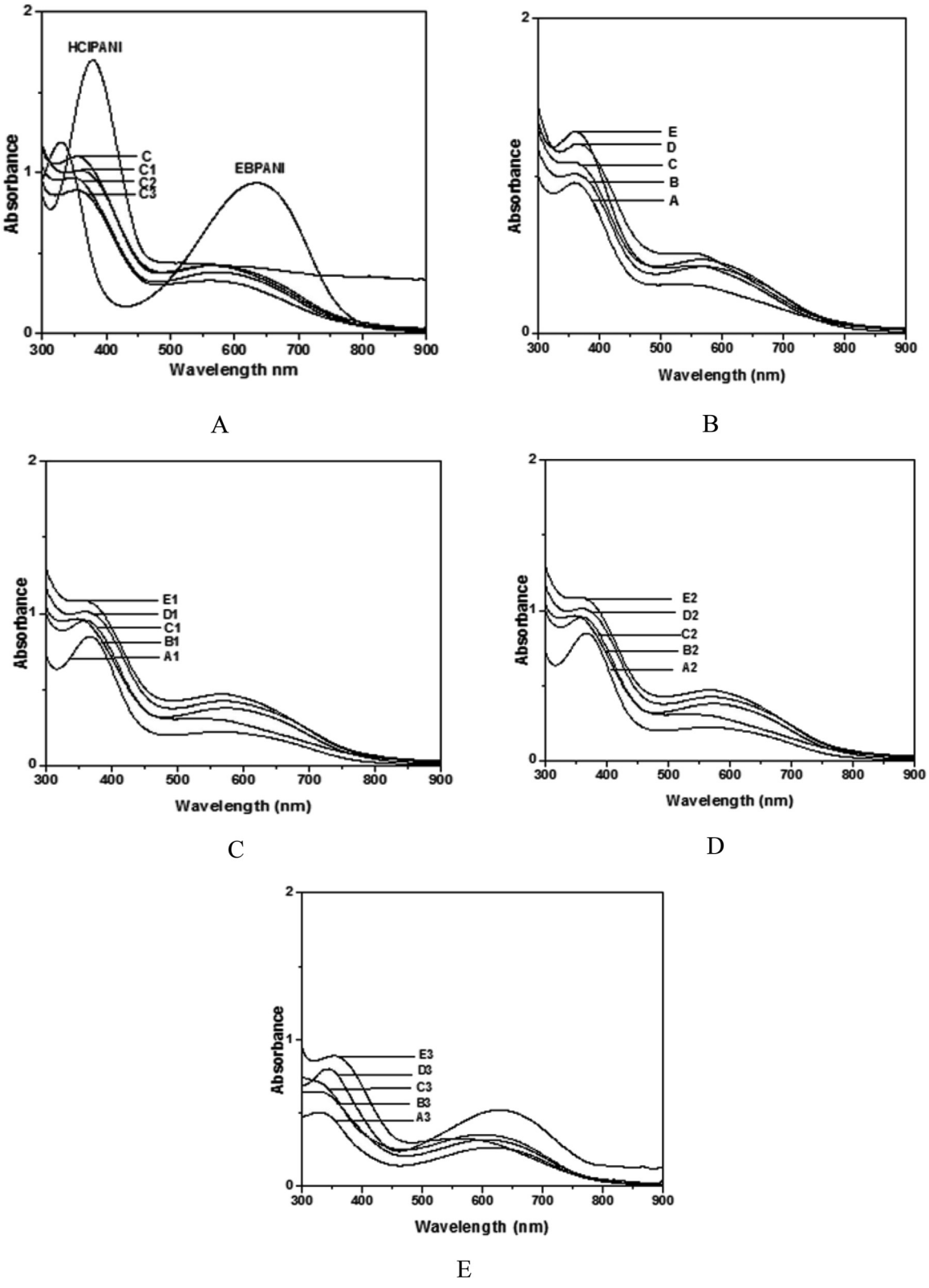

Figure 10: (A) UV–vis spectra of EB-PANI, HCl-PANI C, C_1, C_2 and C_3, (B) PANI doped with $CuSO_4{\cdot}5H_2O$, (C) PANI doped with $[Cu(NH_3)_4]SO_4$, (D) PANI doped with $[Cu(en)_2]SO_4$, (E) f PANI doped with $[Cu(en)_3]SO_4$.

that the strength of this peak intensified as well. A higher doping concentration was achieved as a result of a greater amount of the dopant involved. In a manner that was simultaneous to the increase in conductivity standards, the polaron peak of the intensity increased significantly.

4.7 Conductivity of doped metal salts

Complexes of some transition metal salts $FeSO_4$, $FeCl_3$, $MnCl_2$, $NiCl_2$, $CuCl_2$, $ZnCl_2$, $CdCl_2$, $LaCl_3$, $EuCl_3$, $La(NO_3)_3$, $Eu(NO_3)_3$, $Sm(NO_3)_3$, and $Nd(NO_3)_3$ and polyaniline emeraldine bases were synthesized by UV–vis–IR spectroscopy. There were two distinct instances of severe doping, and they were differentiated by the inorganic salt that was utilized. Films with grain shape, reasonably high conductivities up to 10^{-1} S/cm, and electronic transition spectra that are indicative of both pseudo-proton doping and oxidation of the polymer backbone were produced as a result of the first doping stream. According to the infrared UV–vis spectra or absorption spectra, which were in agreement with the results, the chemical reaction of the benzenoid functional groups of the polymer with the metal cations appeared satisfactory. The second doping regime resulted in a film morphology that was smoother and did not include any grains. However, the film had low conductivity, which generally did not surpass 10^{-3} S/cm, and the solvent content in the film was greater. According to the electronic transition electron and infrared absorption spectrum, the pseudo protonation occurring in the polymer matrix is shown to be reliable. Therefore, based on all the information that was acquired, a model of macromolecular polyaniline transition metal salt–complexes are proposed.[83] The conductivity has been shown to undergo considerable variations over time, which has been the most unexpected aspect of this property.

In most cases, the conductivity of the samples that were created grew by one to two percent over time. The rate of amplitude increased over a few weeks or months, depending on the structure of the film. After that, the conductivity decreased, which may be the result of the typical degradation of the polymeric material. The conductivity had provided more samples that demonstrated that the group of nitrates was much slower in comparison to the films that the first group of dopants doped. Because of this process, the molecules of the solvent are slowly released from the films, which results in a more effective interaction between the dopants and plastic molecules. The spectra of films doped with $NiCl_2$ and $EuCl_3$ salts (Table 3) clearly show the polaron absorption at 440 nm and the absorption tail in the near-IR, which are characteristics of the emeraldine salt form of the polymer.

Table 3: Complex films conductivity S/cm.[6]

EB: HCl	EB: $EuCl_3$	EB: $NiCl_2$	EB: $LaCl_3$	EB: $FeCl_3$
(1×10^{0})	(1×10^{-1})	(4×10^{-2})	(2×10^{-2})	(3×10^{-1})
EB: $CdCl_2$	EB: $Eu(NO_3)_3$	EB: $ZnCl_2$	EB: $Sm(NO_3)_3$	EB: $CuCl_2$
(2×10^{-3})	(4×10^{-3})	(1×10^{-3})	(2×10^{-4})	(3×10^{-4})

Furthermore, the spectra reveal that the polymer has a blue-shifted benzenoid-to-quinoid electronic transition (BQET) at around 550 nm. Copper salt-doped samples exhibited classic characteristics of the polymer's oxidized state, with the exception of a small polaron absorption band that appeared as a shoulder at about 770 nm.[6] It was discovered that the electronic absorption spectra of films changed with time, particularly those doped with the first group of salts. Characteristics of films with greater conductivity have evolved in this direction. As an example, samples doped with $EuCl_3$ and $NiCl_2$ showed a total loss of the BQET band, an enhancement of the polaron absorption characteristics, and a conductivity gain of up to one instruction of greatness during four months. Here, the spectra of PANI films that were acid-protonated or incapacitated by the additional set of salts did not match the final spectra. In addition to suppressing the BQET band, the free-carrier absorption tail in the later films starts at about 500 nm and progressively rises into the infrared region.[84]

5 Conclusions

In conclusion, the incorporation of transition metal salts into polymers is a promising approach that has the potential to modify and advance both the optical and electrical characteristics of these materials. There are a variety of benefits associated with this method, including the ability to modify absorption and emission spectra, enhanced photoluminescence, and the ability to exercise control over color in relation to optical qualities. Enhanced conductivity, greater charge carrier mobility, and the capacity to control the band gap are all beneficial to the electrical characteristics of the material at the same time. These technological breakthroughs have major consequences for an extensive variety of requests, including organic solar cells, sensors, flexible electronics, and optoelectronic devices, amongst others. Because of their flexibility, transition metal salts make it possible to fine-tune the characteristics of materials in order to fulfill certain needs associated with a variety of technical areas. In addition, the enhancements in stability and durability that are brought about by doping are a

significant contributor to the long-term dependability of devices that are based on polymers.

Research ethics: Not applicable.
Author contributions: The authors have accepted responsibility for the entire content of this manuscript and approved its submission.
Competing interests: The authors state no conflict of interest.
Research funding: None declared.
Data availability: Not applicable.

References

1. Cox, P. A. *Transition Metal Oxides: An Introduction to their Electronic Structure and Properties*; Oxford University Press: Oxford, 2010.
2. Saha, S.; Samanta, P.; Murmu, N. C.; Kuila, T. A Review on the Heterostructure Nanomaterials for Supercapacitor Application. *J. Energy Storage* **2018**, *17*, 181–202.
3. Omer, R. A.; Hughes, A.; Hama, J. R.; Wang, W.; Tai, H. Hydrogels from Dextran and Soybean Oil by UV Photo-polymerization. *J. Appl. Polym. Sci.* **2015**, *132*. https://doi.org/10.1002/app.41446.
4. Omer, R. A.; Hama, J. R.; Rashid, R. S. M. The Effect of Dextran Molecular Weight on the Biodegradable Hydrogel with Oil, Synthesized by the Michael Addition Reaction. *Adv. Polym. Technol.* 2017, *36*, 120–127.
5. Tumma, M.; Srivastava, R. Transition Metal Nanoparticles Supported on Mesoporous Polyaniline Catalyzed Reduction of Nitroaromatics. *Catal. Commun.* **2013**, *37*, 64–68.
6. Dimitriev, O. Doping of Polyaniline by Transition-Metal Salts. *Macromolecules* **2004**, *37*, 3388–3395.
7. Wang, T.; Chen, H. C.; Yu, F.; Zhao, X.; Wang, H. Boosting the Cycling Stability of Transition Metal Compounds-Based Supercapacitors. *Energy Storage Mater.* **2019**, *16*, 545–573.
8. Zhang, A.; Liang, Y.; Zhang, H.; Geng, Z.; Zeng, J. Doping Regulation in Transition Metal Compounds for Electrocatalysis. *Chem. Soc. Rev.* **2021**, *50*, 9817–9844.
9. List, B. *Introduction: Organocatalysis*; ACS Publications: Washington, D.C., 2007; pp 5413–5415.
10. Italiano, C.; Bizkarra, K.; Barrio, V.; Cambra, J.; Pino, L.; Vita, A. Renewable Hydrogen Production via Steam Reforming of Simulated Bio-Oil over Ni-Based Catalysts. *Int. J. Hydrogen Energy* **2019**, *44*, 14671–14682.
11. Ren, J.; Liu, Y.-L.; Zhao, X.-Y.; Cao, J.-P. Biomass Thermochemical Conversion: A Review on Tar Elimination from Biomass Catalytic Gasification. *J. Energy Inst.* **2020**, *93*, 1083–1098.
12. Ahmed, A. A. A.; Al-Hussam, A. M.; Abdulwahab, A. M.; Ahmed, A. The Impact of Sodium Chloride as Dopant on Optical and Electrical Properties of Polyvinyl Alcohol. *AIMS Mater. Sci.* **2018**, *5*, 533–542.
13. Drandova, G. I. *NMR Investigations in Copper-Oxide Chain Compounds and High-T (C) Superconductors*; The University of Texas at Austin: Austin, 2001.
14. Hoa, N. D.; An, S. Y.; Dung, N. Q.; Van Quy, N.; Kim, D. Synthesis of P-type Semiconducting Cupric Oxide Thin Films and Their Application to Hydrogen Detection. *Sensor. Actuator. B Chem.* **2010**, *146*, 239–244.
15. Chianelli, R. R.; Siadati, M. H.; De la Rosa, M. P.; Berhault, G.; Wilcoxon, J. P.; Bearden Jr, R.; Abrams, B. L. Catalytic Properties of Single Layers of Transition Metal Sulfide Catalytic Materials. *Catal. Rev.* **2006**, *4*, 81–41.
16. Ejigu, A.; Fujisawa, K.; Spencer, B. F.; Wang, B.; Terrones, M.; Kinloch, I. A.; Dryfe, R. A. On the Role of Transition Metal Salts during Electrochemical Exfoliation of Graphite: Antioxidants or Metal Oxide Decorators for Energy Storage Applications. *Adv. Funct. Mater.* **2018**, *28*, 1804357.
17. N'Tsoukpoe, K. E.; Rammelberg, H. U.; Lele, A. F.; Korhammer, K.; Watts, B. A.; Schmidt, T.; Ruck, W. K. A Review on the Use of Calcium Chloride in Applied Thermal Engineering. *Appl. Therm. Eng.* **2015**, *75*, 513–531.
18. Thoruwa, T.; Smith, J.; Grant, A.; Johnstone, C. Developments in Solar Drying Using Forced Ventilation and Solar Regenerated Desiccant Materials. *Renew. Energy* **1996**, *9*, 686–689.
19. Wang, L.; Wang, R.; Xia, Z.; Wu, J. Studies on Heat Pipe Type Adsorption Ice Maker for Fishing Boats. *Int. J. Refrig.* **2008**, *31*, 989–997.
20. Tyagi, V.; Buddhi, D. Thermal Cycle Testing of Calcium Chloride Hexahydrate as a Possible PCM for Latent Heat Storage. *Sol. Energy Mater. Sol. Cell.* **2008**, *92*, 891–899.
21. Miyazaki, T.; Akisawa, A.; Saha, B.; El-Sharkawy, I.; Chakraborty, A. A New Cycle Time Allocation for Enhancing the Performance of Two-Bed Adsorption Chillers. *Int. J. Refrig.* **2009**, *32*, 846–853.
22. Bansal, P.; Jain, S.; Moon, C. Performance Comparison of an Adiabatic and an Internally Cooled Structured Packed-Bed Dehumidifier. *Appl. Therm. Eng.* **2011**, *31*, 14–19.
23. Bignozzi, C.; Argazzi, R.; Boaretto, R.; Busatto, E.; Carli, S.; Ronconi, F.; Caramori, S. The Role of Transition Metal Complexes in Dye Sensitized Solar Devices. *Coord. Chem. Rev.* **2013**, *257*, 1472–1492.
24. Wilkinson, G.; Gillard, R. D.; McCleverty, J. A. *Comprehensive Coordination Chemistry. the Synthesis, Reactions, Properties and Applications of Coordination Compounds. V. 3. Main Group and Early Transition Elements*; Pergamon Press: Oxford, 1987.
25. Xia, H.; Zhang, C.; Qiu, S.; Lu, P.; Zhang, J.; Ma, Y. Highly Efficient Red Phosphorescent Light-Emitting Diodes Based on Ruthenium (II)-Complex-Doped Semiconductive Polymers. *Appl. Phys. Lett.* **2004**, *8*, 4290–4292.
26. Rudmann, H.; Shimada, S.; Rubner, M. F. Operational Mechanism of Light-Emitting Devices Based on Ru (II) Complexes: Evidence for Electrochemical Junction Formation. *J. Appl. Phys.* **2003**, *94*, 115–122.
27. Kapturkiewicz, A. Electrogenerated Chemiluminescence from the Tris (4, 7-diphenyl-1, 10-phenanthroline) Ruthenium (II) Complex. *Chem. Phys. Lett.* **1995**, *236*, 389–394.
28. Marusak, R. A.; Doan, K.; Cummings, S. D. *Integrated Approach to Coordination Chemistry: An Inorganic Laboratory Guide*; John Wiley & Sons: Hoboken, NJ, 2007.
29. Miguel, P. J. S.; Roitzsch, M.; Yin, L.; Lax, P. M.; Holland, L.; Krizanovic, O.; Lutterbeck, M.; Schürmann, M.; Fusch, E. C.; Lippert, B. On the Many Roles of NH_3 Ligands in Mono-and Multinuclear Complexes of Platinum. *Dalton Trans.* **2009**, 10774–10786. https://doi.org/10.1039/b916537a.
30. Tong, M.-L.; Chen, X.-M. Synthesis of Coordination Compounds and Coordination Polymers. *Mod. Inorg. Synth. Chem.* **2017**, 189–217. https://doi.org/10.1016/b978-0-444-63591-4.00008-2.
31. Preetz, W.; Peters, G.; Bublitz, D. Preparation and Spectroscopic Investigations of Mixed Octahedral Complexes and Clusters. *Chem. Rev.* **1996**, *96*, 977–1026.
32. Nadr, R.; Abdulrahman, B.; Omer, R. Various Flavone Types: A Study of Synthesis Approaches and their Antioxidant Properties (A Review). *Russ. J. Gen. Chem.* **2023**, *93*, 3188–3199.
33. Bailey, K. C.; Morgan, G.; Wardlaw, W.; Moody, G. T.; Mills, W. Obituary Notices: James Bell, 1899–1941; Sir Gilbert Morgan, 1870–1940; Sir

William J. Pope, 1870–1939. *J. Chem. Soc.* **1941**, 689–715. https://doi.org/10.1039/jr9410000689.
34. Anderson, J. R.; Chapman, S. K. Ligand Probes for Heme Proteins. *Dalton Trans.* **2005**, 13–24. https://doi.org/10.1039/b413046d.
35. Gokel, G. W.; Leevy, W. M.; Weber, M. E. Crown Ethers: Sensors for Ions and Molecular Scaffolds for Materials and Biological Models. *Chem. Rev.* **2004**, *104*, 2723–2750.
36. Nast, R. Coordination Chemistry of Metal Alkynyl Compounds. *Coord. Chem. Rev.* **1982**, *47*, 89–124.
37. Nast, R.; Sirtl, E. Alkinyloverbindungen von übergangsmetallen, III. Mitteil. 1): Hexaalkinylokomplexe von Chrom (III). *Chem. Ber.* **1955**, *88*, 1723–1726.
38. Nast, R.; Griesshammer, H. Alkinyloverbindungen von Übergangsmetallen, IX. Alkinylokomplexe von Mangan (II). *Chem. Ber.* **1957**, *90*, 1315–1320.
39. Nast, R.; Müller, H. P. Alkinylverbindungen von Übergangsmetallen, XXXIV: IR-Spektroskopische Untersuchungen von Tetrakis (alkinyl)-manganaten (II). *Chem. Ber.* **1978**, *111*, 415–416.
40. Nast, R.; Urban, F. Alkinyloverbindungen von übergangsmetallen. VI. Alkinylokomplexe von Eisen (II) und Eisen (III). *Z. Anorg. Allg. Chem.* **1956**, *287*, 17–23.
41. Rojas, E.; Santos, A.; Moreno, V.; Del Pino, C. Cyclohexylethynyl Complexes of CoII and FeII. *J. Organomet. Chem.* **1979**, *181*, 365–373.
42. Nast, R.; Lewinsky, H. Alkinyloverbindungen von Übergangsmetallen. IV. Alkinylokomplexe von Kobalt (II) und Kobalt (III). *Z. Anorg. Allg. Chem.* **1955**, *282*, 210–216.
43. Nast, R.; Fock, K. Alkinylverbindungen von Übergangsmetallen, XXX1) Hexaalkinylcobaltate (II). *Chem. Ber.* **1976**, *109*, 455–458.
44. Barral, M.; Jimenez, R.; Royer, E.; Moreno, V.; Santos, A. σ-Acetylides of Ni (II), Pd (II), and Pt (II). *Inorg. Chim. Acta.* **1978**, *31*, 165–169.
45. Taube, R., Honymus, G. (**1975**) Lithium-Tetraphenyl-und-Tetramethyl-Niccolat (II). *Angew. Chem. 87*, 291.
46. Nast, R.; Pfab, W. Alkinyloverbindungen von Übergangsmetallen, V. Mitteil.: Alkinylokomplexe von Kupfer. *Chem. Ber.* **1956**, *89*, 415–421.
47. Nast, R.; Müller, R. Alkinyloverbindungen von Übergangsmetallen, XIII. Über einen Äthinylokomplex des Zinks. *Chem. Ber.* **1958**, *91*, 2861–2865.
48. Nast, R.; Schindel, H. Alkinylverbindungen von Übergangsmetallen. XXI. Komplexe Acetylide von Silber. *Z. Anorg. Allg. Chem.* **1963**, *326*, 201–208.
49. Yeşilel, O. Z.; İlker, İ.; Soylu, M. S.; Darcan, C.; Süzen, Y. Synthesis, Crystal Structures and Antimicrobial Properties of Copper (II)-Thiophene-2, 5-dicarboxylate Complexes with N-Donor Ligands. *Polyhedron* **2012**, *39*, 14–3924.
50. Sharpe, A. G. *The Chemistry of Cyano Complexes of the Transition Metals*; Academic Press: London, 1976.
51. Back, S.; Rheinwald, G.; Zsolnai, L.; Huttner, G.; Lang, H. Synthesis, Reaction Chemistry and Electrochemical Behaviour of (η5–$C_5H_4SiMe_3)_2Hf$ (C·CFc)$_2$. *J. Organomet. Chem.* **1998**, *563*, 73–79.
52. West, C. Diffraction of X-Rays by a Linear Crystal Grating of AgCN. *Z. für Kristallogr. – Cryst. Mater.* **1935**, *90*, 555–558.
53. Nast, R.; Beck, G. Alkinylverbindungen vn Übergangsmetallen, XVIII1) Zur Existenz von Alkinyl-pentacyanoferraten. *Chem. Ber.* **1962**, *95*, 2161–2165.
54. Nast, R.; Fock, K. Alkinylverbindungen von Übergangsmetallen, XXXII. Komplexe von Alkinylverbindungen des Cobalts (II) mit tertiären Phosphinen. *Chem. Ber.* **1977**, *110*, 280–284.
55. Nast, R.; Hörl, W. Alkinylverbindungen von Übergangsmetallen, XV. Komplexe Acetylide von Palladium (II) und Palladium (0). *Chem. Ber.* **1962**, *95*, 1470–1477.
56. Nast, R.; Voß, J.; Kramolowsky, R. Alkinylverbindungen von Übergangsmetallen, XXIX. Alkinyl [1, 2-bis (diphenylphosphino) äthan]-Komplexe des Platins (II). *Chem. Ber.* **1975**, *108*, 1511–1517.
57. Nasl, R.; Krüger, K.; Beck, G. Alkinylverbindungen von Übergangsmetallen. XXVII. Über die Reaktion von $K_2[Fe(CN)_5NO]$ mit Kaliumphenylacetylid. *Z. Anorg. Allg. Chem.* **1967**, *350*, 177–185.
58. Atwood, J. L.; Hunter, W. E.; Wayda, A. L.; Evans, W. J. Synthesis and Crystallographic Characterization of a Dimeric Alkynide-Bridged organolanthanide:$[(C_5H_5)_2$ErC.ident.CC$(CH_3)_3]_2$. *Inorg. Chem.* **1981**, *20*, 4115–4119.
59. Nast, R.; Käb, K. Alkinylverbindungen des thalliums. *J. Organomet. Chem.* **1966**, *6*, 456–463.
60. Nast, R.; Köhl, H. Alkinylverbindungen von Übergangsmetallen, XXIII. Trialkinyltricarbonylkomplexe von Molybdän (0) und Wolfram (0). *Chem. Ber.* **1964**, *97*, 207–211.
61. Ding, P.; Lin, Z.; Guo, X.; Wu, L.; Wang, Y.; Guo, H.; Li, L.; Yu, H. Polymer Electrolytes and Interfaces in Solid-State Lithium Metal Batteries. *Mater. Today* **2021**, *51*, 449–474.
62. Armand, M. Polymer Solid Electrolytes-An Overview. *Solid State Ionics* **1983**, *9*, 745–754.
63. Wang, L.; Zhong, Y.; Wen, Z.; Li, C.; Zhao, J.; Ge, M.; Zhou, P.; Zhang, Y.; Tang, Y.; Hong, G. A Strong Lewis Acid Imparts High Ionic Conductivity and Interfacial Stability to Polymer Composite Electrolytes towards All-Solid-State Li-Metal Batteries. *Sci. China Mater.* **2022**, *65*, 2179–2188.
64. Xue, Z.; He, D.; Xie, X. Poly (Ethylene Oxide)-Based Electrolytes for Lithium-Ion Batteries. *J. Mater. Chem. A* **2015**, *3*, 19218–19253.
65. Angell, C.; Liu, C.; Sanchez, E. Rubbery Solid Electrolytes with Dominant Cationic Transport and High Ambient Conductivity. *Nature* **1993**, *362*, 137–139.
66. Young, W. S.; Kuan, W. F.; Epps III, T. H. Block Copolymer Electrolytes for Rechargeable Lithium Batteries. *J. Polym. Sci. B Polym. Phys.* **2014**, *52*, 1–16.
67. Kumar, A.; Sivaprahsam, D.; Thakur, A. D. Improvement of Thermoelectric Properties of Lanthanum Cobaltate by Sr and Mn Co-Substitution. *J. Alloys Compd.* **2018**, *735*, 1787–1791.
68. Li, C.; Qin, B.; Zhang, Y.; Varzi, A.; Passerini, S.; Wang, J.; Dong, J.; Zeng, D.; Liu, Z.; Cheng, H. Single-ion Conducting Electrolyte Based on Electrospun Nanofibers for High-Performance Lithium Batteries. *Adv. Energy Mater.* **2019**, *9*, 1803422.
69. Strauss, E.; Menkin, S.; Golodnitsky, D. On the Way to High-Conductivity Single Lithium-Ion Conductors. *J. Solid State Electrochem.* **2017**, *21*, 1879–1905.
70. Battle, A. R.; Choi, R.; Hibbs, D. E.; Hambley, T. W. Platinum (IV) Analogues of AMD_{473} (cis-[$PtCl_2$ (NH_3)(2-picoline)]): Preparative, Structural, and Electrochemical Studies. *Inorg. Chem.* **2006**, *45*, 6317–6322.
71. McBrien, D.; Slater, T. F. *Biochemical Mechanisms of Platinum Antitumour Drugs: Based on the Proceedings of a Symposium held at Brunel University, 3–5th July 1985*; Oxford University Press: Oxford, 1986.
72. Nicolini, M. *Platinum and Other Metal Coordination Compounds in Cancer Chemotherapy: Proceedings of the Fifth International Symposium on Platinum and Other Metal Coordination Compounds in Cancer Chemotherapy Abano, Padua, Italy—June 29–July 2, 1987*; Springer Science & Business Media: New York, 2012.
73. Nayak, P.; Sudhakar, Y.; De, S.; Ismayil; Shetty, S. K.; Cyriac, V. Modifying the Microstructure of Chitosan/methylcellulose Polymer Blend via Magnesium Nitrate Doping to Enhance its Ionic Conductivity for Energy Storage Application. *Cellulose* **2023**, *30*, 4401–4419.

74. Dana, A. T. Effect of $CuCl_2$ Powder on the Optical Characterization of Methylcellulose (MC) Polymer Composite. *Alex. Eng. J.* **2022**, *61*, 2354–2365.
75. Sauerheber, R.; Heinz, B. Temperature Effects on Conductivity of Seawater and Physiologic Saline, Mechanism and Significance. *Chem. Sci. J.* **2015**, *6*, 4172.
76. Chen, C.; Yang, C. Synthesis, Characterisation and Properties of Polyanilines Containing Transition Metal Ions. *Synth. Met.* **2005**, *15*, 3133–3136.
77. Higuchi, M.; Imoda, D.; Hirao, T. Redox Behavior of Polyaniline – Transition Metal Complexes in Solution. *Macromolecules* **1996**, *29*, 8277–8279.
78. Virji, S.; Fowler, J. D.; Baker, C. O.; Huang, J.; Kaner, R. B.; Weiller, B. H. Polyaniline Nanofiber Composites with Metal Salts: Chemical Sensors for Hydrogen Sulfide. *Small* **2005**, *1*, 624–627.
79. Amarnath, C. A.; Kim, J.; Kim, K.; Choi, J.; Sohn, D. Nanoflakes to Nanorods and Nanospheres Transition of Selenious Acid Doped Polyaniline. *Polymer* **2008**, *49*, 432–437.
80. Neelgund, G. M.; Oki, A. A Facile Method for the Synthesis of Polyaniline Nanospheres and the Effect of Doping on their Electrical Conductivity. *Polym. Int.* **2011**, *60*, 1291–1295.
81. Šeděnková, I.; Trchová, M.; Stejskal, J. Thermal Degradation of Polyaniline Films Prepared in Solutions of Strong and Weak Acids and in Water–FTIR and Raman Spectroscopic Studies. *Polym. Degrad. Stabil.* **2008**, *93*, 2147–2157.
82. Gizdavic-Nikolaidis, M.; Travas-Sejdic, J.; Cooney, R.; Bowmaker, G. Spectroscopic Studies of Interactions of Polyaniline with Some Cu (II) Compounds. *Curr. Appl. Phys.* **2006**, *6*, 457–461.
83. Leng, J.; McCall, R.; Cromack, K.; Sun, Y.; Manohar, S.; MacDiarmid, A.; Epstein, A. Photoexcited Solitons and Polarons in Pernigraniline-Base Polymers. *Phys. Rev. B* **1993**, *48*, 15719.
84. Wudl, F.; Angus Jr., R.; Lu, F.; Allemand, P.; Vachon, D.; Nowak, M.; Liu, Z.; Schaffer, H.; Heeger, A. Poly-p-phenyleneamineimine: Synthesis and Comparison to Polyaniline. *J. Am. Chem. Soc.* **1987**, *109*, 3677–3684.